





Article

Application of the Integrated Supercritical Fluid Extraction–Impregnation Process (SFE-SSI) for Development of Materials with Antiviral Properties

Ivana Lukic ^{1,*}, Jelena Pajnik ², Jakov Nisavic ³, Vanja Tadic ⁴, Erika Vági ⁵, Edit Szekely ⁵ and Irena Zizovic ^{6,*}

- ¹ Faculty of Technology and Metallurgy, University of Belgrade, Karnegijeva 4, 11120 Belgrade, Serbia
² Innovation Center of the Faculty of Technology and Metallurgy, University of Belgrade, Karnegijeva 4, 11200 Belgrade, Serbia; jpajnik@tmf.bg.ac.rs
³ Faculty of Veterinary Medicine, University of Belgrade, Bulevar Oslobođenja 18, 11000 Belgrade, Serbia; jakovmoni@vet.bg.ac.rs
⁴ Institute for Medical Plant Research “Dr Josif Pancic”, Tadeusa Koscuska 1, 11000 Belgrade, Serbia; vtadic@mocbilja.rs
⁵ Department of Chemical and Environmental Process Engineering, Budapest University of Technology and Economics, H-1521 Budapest, Hungary; vagi.erika.maria@vbk.bme.hu (E.V.); sz-edit@mail.bme.hu (E.S.)
⁶ Faculty of Chemistry, Wrocław University of Science and Technology, Wybrzeże Wyspińskiego 27, 50-370 Wrocław, Poland
* Correspondence: ilukic@tmf.bg.ac.rs (I.L.); irena.zizovic@pwr.edu.pl (I.Z.); Tel.: +38-1113303709 (I.L.)



Citation: Lukic, I.; Pajnik, J.; Nisavic, J.; Tadic, V.; Vági, E.; Szekely, E.; Zizovic, I. Application of the Integrated Supercritical Fluid Extraction–Impregnation Process (SFE-SSI) for Development of Materials with Antiviral Properties. *Processes* **2022**, *10*, 680. <https://doi.org/10.3390/pr10040680>

Academic Editor: Maria Angela A. Meireles

Received: 26 February 2022

Accepted: 29 March 2022

Published: 31 March 2022

Publisher’s Note: MDPI stays neutral with regard to jurisdictional claims in published maps and institutional affiliations.



Copyright: © 2022 by the authors. Licensee MDPI, Basel, Switzerland. This article is an open access article distributed under the terms and conditions of the Creative Commons Attribution (CC BY) license (<https://creativecommons.org/licenses/by/4.0/>).

Abstract: The integrated supercritical fluid extraction–impregnation process (SFE-SSI) was performed to fabricate material with antiviral properties against the herpes simplex virus (HSV). Cotton gauze and starch/chitosan polymer films (SCF) were impregnated with components extracted from *Melissa officinalis* at 10 MPa and 40 °C using a green medium, supercritical carbon dioxide (scCO₂). The influences of the processing mode regarding the flow of the supercritical fluid through the system, and the mass ratio of the plant material and the solid carrier, on the impregnation yield of *M. officinalis* extract were studied. The results revealed that the introduction of a fresh amount of CO₂ into the system enabled the highest impregnation yield of 2.24% for cotton gauze and 8.71% for SCF. The presence of *M. officinalis* extract on the surface of both impregnated cotton gauze and SCF was confirmed by FTIR and GC analyses after the re-extraction of the impregnated samples. The *M. officinalis* impregnated materials showed a strong inhibitory effect against Bovine herpesvirus type 1 (BHV-1).

Keywords: *Melissa officinalis*; supercritical extraction; supercritical impregnation; antiviral activity

1. Introduction

Herpes simplex virus (HSV) is a pathogen member of the large *Herpesviridae* family, with the ability to establish a latent infection in the nervous system that can be reactivated, causing recurrent infections, whose frequency and severity mostly depend on the host’s immune status [1,2]. Type 1 (HSV-1) causes primary infections presented clinically as herpes labialis, with common areas of infection being face, lips, and mouth cavity, whereas infections caused by type 2 (HSV-2) affect the genital area; however, this type also causes neonatal infections and fatal infections such as meningitis and cervical cancer [3,4].

During recent decades, scientific research interest to design antimicrobial agents from plants has increased, due to these agents’ low side effects, low costs of production, and the fact that they do not contribute to further resistance of microbes. A large number of anti-herpes screening experiments on medicinal plant extracts have been reported [5,6], with a significant contribution of *Melissa officinalis*, commonly known as lemon balm, a perennial lemon-scented herb native to the eastern Mediterranean region and western Asia [3,7,8]. In addition to its well-proven antibacterial and antifungal activity [9], *M.*

officinalis plant extract has been reported to possess antiviral activity against several viruses, including HSV, both type 1 and 2 [3,4,7–12].

Considering the lipophilic nature of lemon balm essential oil, which enables it to penetrate the skin, *M. officinalis* oil may be suitable for topical treatment of herpetic infections [3]. Natural-based, biodegradable, and biocompatible materials are the most suitable carriers of active compounds in transdermal systems. Cotton gauze, a material that meets the aforementioned requirements, is widely used for hygienic purposes due to its natural softness, high hygroscopicity, and heat-retaining properties [13]. Starch and chitosan are among the most abundant naturally occurring polysaccharides, derived from renewable resources, and their blend can form a biodegradable polymer film with high durability, good biocompatibility, and low toxicity [14].

Most of the studies reporting *M. officinalis* antiviral activity utilized extracts obtained either in the process of hydrodistillation, usually performed at high temperatures, thus having high energy demands, and causing potential hydrolysis or thermal degradation of the most sensitive compounds; or with the use of organic solvents that can lower the purity of the extract. These drawbacks can be significantly reduced using supercritical fluid technology, which has been recognized as a promising ‘green’ alternative method to conventional processes for various applications [15,16]. Supercritical fluid extraction (SFE), with supercritical carbon dioxide (scCO₂) as the most commonly used supercritical fluid, is a green process in which scCO₂ is easily removed from the extract by decompression, enabling the production of solvent-free and highly valued plant extracts [15,17,18]. Properties of scCO₂, especially its high diffusion ability, also make it suitable for incorporation of the compounds soluble in scCO₂ into the solid matrix [13,16]. Supercritical solvent impregnation (SSI) allows the production of solvent-free materials with high purity and a homogeneous distribution of natural products inside the carrier in shorter processing times, compared to conventional processes. The SSI process is a widely employed technique in different areas, used as a processing aid for the creation of novel materials with different end applications, such as in the pharmaceutical, biomedical, food, and textile industries [19–23]. This technique was successfully applied to impregnate a variety of substances, including essential oils (oregano, lavandin, clove, cinnamon), mango leaf extract, caffeine, and α -tocopherol, onto different materials [24–30].

The integrated SFE-SSI process, which merges SFE and SSI into one process, was recently introduced [31], and its feasibility was later tested in a few studies [32–36]. By coupling the extraction and the impregnation processes, the loss of the extract in the tubes, vessels, and other parts of the equipment is minimized since the scCO₂-extract solution leaving the extractor vessel is directly used for the impregnation. Moreover, the intermediate decompression step in the separate SFE and SSI processes is avoided, leading to energy and time savings.

Only a few reports on SFE of *M. officinalis* are found in the literature [37–41], and fewer deal with the SFE at lower pressures aimed at essential oil isolation and the extract characterization [37,39]. To the best of our knowledge, there are no available data on SSI of *M. officinalis* extract, or the integrated SFE-SSI process, for incorporation of balm extract into a solid carrier.

The main goal of this study was to obtain functionalized material with a potential for the treatment of HSV-1 infections using the integrated SFE-SSI process. Cotton gauze and polymer films based on starch and chitosan were impregnated with components extracted from *M. officinalis* at 10 MPa and 40 °C. The influences of different processing modes, and the mass ratio of plant material and the used carrier, on the obtained impregnation yield were studied. The antiviral potential of the obtained materials against HSV-1 was evaluated. To the best of our knowledge, there are no data on the anti-herpes activity of materials impregnated with *M. officinalis* extracts. The chemical composition of *M. officinalis* extract obtained in the SFE process, and the re-extracts from impregnated materials, were determined using GC/MS and HPLC techniques.

2. Materials and Methods

2.1. Materials

Melissa officinalis folium (Serbia, identified at the Institute for Medicinal Plant Research “Dr Josif Pancic”, Belgrade) was milled in a blender and sieved just before the SFE. Commercial CO₂ (purity 99%) was purchased from Messer-Tehnogas, Serbia, and liquid food-grade CO₂ (99.99%) from Biogon C., Linde Ltd., Budapest, Hungary. Sterile cotton gauze with a weaving density of 17 threads/cm² was produced by Niva, Serbia. Corn starch (amylose content 28%) was obtained from Starch Industry Jabuka (Serbia). Chitosan with high molecular weight (310,000–375,000 g/mol, 75–85% deacetylated), and rosmarinic acid (standard for HPLC, ≥98%) were purchased from Sigma-Aldrich Chemie GmbH, Steinheim, Germany.

Reference BPT-1 strain of Bovine herpesvirus 1 (BHV-1) (Department of Microbiology, Faculty of veterinary medicine University of Belgrade), titer 7.00 TCID₅₀/0.1 mL, served as a control during the examination. Rabbit kidney-13 cells (RK-13, ATCC CCL-37, IZSBS, Brescia, Italy) were grown in minimum essential medium-Eagle MEM (Sigma Inc., Marlborough, MA, USA), containing penicillin 100 U/mL (Galenika, Belgrade, Serbia), streptomycin 100 µg/mL (Galenika, Belgrade, Serbia), fungizone 25 µg/mL (Serva, Heidelberg, Germany), and 10% fetal calf sera (Sigma Inc., Marlborough, MA, USA). The flasks with RK-13 cells were incubated at 37 °C with a 5% CO₂ air atmosphere. The propagation of BHV-1 reference strain BPT-1 and determination of the virus infectivity titer were performed in RK-13 cell line.

2.2. Starch-Chitosan Film (SCF) Preparation

The 1% (*w/v*) starch solution was prepared by dispersing 1 g of starch in 100 mL of distilled water and heating the mixture on a hotplate for 10 min at 90 °C with stirring. A quantity of 1 g of chitosan was dissolved in 100 mL of 2% (*w/v*) acetic acid solution to yield a 1% (*w/v*) chitosan solution. SCF was prepared by mixing the starch solution (1% *w/v*) with the chitosan solution (1% *w/v*) in a mass ratio of 1:1 (*w/w*) and the addition of 0.5 g of glycerol (25% (*w/w*) of the total solid weight) [42]. After cooling to room temperature, about 45 g of the blended solution was cast onto a 120 mm × 55 mm mold. After drying the films at room temperature for at least 72 h, they were dried at 50 °C for 24 h prior to testing.

2.3. Supercritical Fluid Extraction (SFE)

Selection of operating conditions of scCO₂ extraction, primary temperature, and pressure was based on previous reports, which show that, for isolation of volatile compounds, i.e., essential oils proven to possess antiviral activity [4], mild pressures (from 9 to 10 MPa) and temperatures (from 40 to 50 °C) were optimal [15]. Therefore, extraction of *M. officinalis* was performed at a temperature of 40 °C and pressure of 10 MPa.

2.3.1. Laboratory Scale Extraction

The scCO₂ extraction was performed separately in the extraction vessel (280 mL) of the laboratory scale unit of the combined SFE-SSI process, described in Section 2.4. The initial mass of the plant material used for continuous extraction was 50 ± 2.0 g. The average extraction time was 3 h, and the CO₂ flow rate was 0.66 kg/h. The experiments were performed in triplicate.

2.3.2. Pilot Scale Extraction

The supercritical carbon dioxide extraction was carried out in a pilot plant apparatus with a 5 L high-pressure extraction vessel (supplied by Natex, Ternitz, Austria) equipped with two separation vessels in series; a detailed description is provided elsewhere [43]. A quantity of 1000 g (±5.0 g) of ground lemon balm was loaded into the basket of the extraction vessel and the flow rate of scCO₂ was set at 7 kg/h. Two separators were connected to the extraction vessel. Both separators were set at 40 °C, while the pressure of the first separator was higher (4 MPa) than that of the second separator (2 MPa). The

extractions ran in batches; therefore, CO₂ was not recycled. According to the moisture content of the actual plant material, water was co-extracted and decanted. The moisture-free crude extracts were weighed and the yield was calculated as g dry extract/100 g dry material (% w/w).

2.4. Integrated Supercritical Fluid Extraction–Impregnation Process (SFE-SSI)

The integrated process of supercritical fluid extraction of *M. officinalis* extract and its impregnation on the carrier (cotton gauze or SCF) was performed using a laboratory scale unit (High Pressure Extraction Adsorption (HPEA) 500, Eurotechnica, Bargteheide, Germany), as presented in Figure 1 and described in detail elsewhere [33,35].

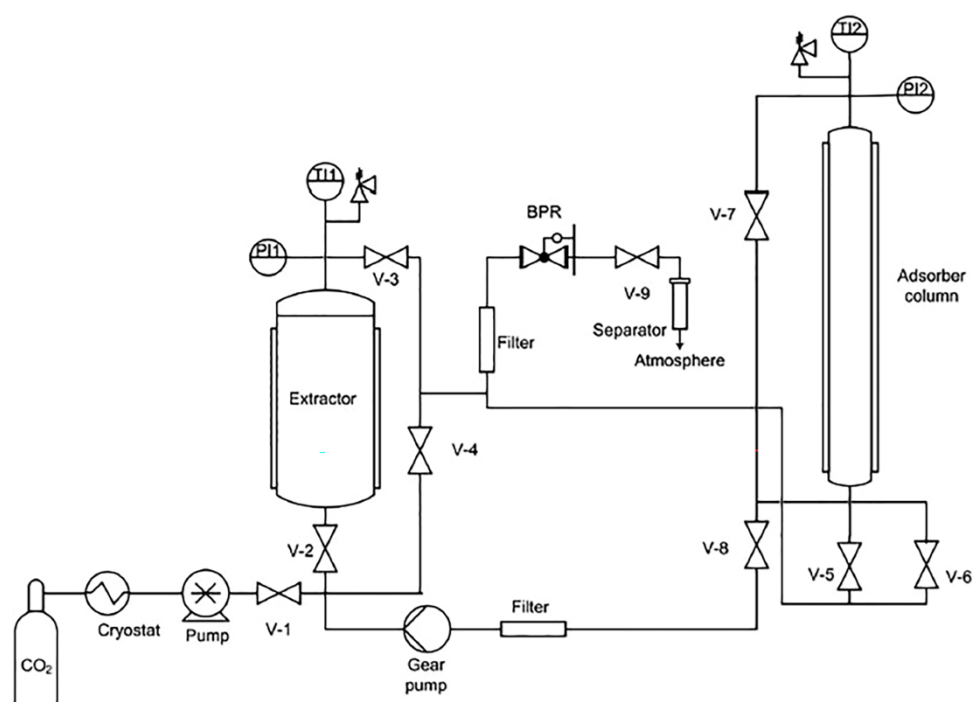


Figure 1. Schematic presentation of the HPEA 500 unit.

Briefly, the extractor vessel (280 mL) was filled with milled balm plant material, while cotton gauze was rolled and placed in the adsorption column (100 mL). SCF was rolled and placed in the porous basket at the top of the column. In experiments, where not indicated otherwise, the plant to carrier mass ratio (m_p/m_c) was 25 and the mass of plant (m_p) was 50 ± 2.0 g. Once the desired temperature was reached, CO₂ was pumped into the system until process pressure was reached in the entire system. Circulation of solution (CO₂ + extract) through both vessels was provided using the high-pressure gear pump. In this way the solution comes in contact with the gauze or SCF and impregnation is carried out. In all experiments, the operating pressure and temperature were 10 MPa and 40 °C in the entire system. Four processing modes were applied in SFE-SSI experiments:

Mode I: After reaching process conditions (pressure and temperature), the CO₂ + extract solution circulated through the system for 5 h.

Mode II: Three cycles of circulation of the CO₂ + extract solution through the system were applied. In the first two cycles the solution circulated for 2 h, and in the third cycle for 1 h. Between the cycles, fresh CO₂ was introduced into the system at a flow rate of 10 g/min for 5 min.

Modes III and IV were performed in five and seven cycles, respectively. Each cycle lasted for 1 h. After each cycle, fresh CO₂ was introduced into the system at a flow rate of 10 g/min for 5 min.

After the last cycle, in all modes, CO₂ was released from the system at a decompression rate of 1 MPa/min.

To obtain the highest impregnation yields for selected carriers, the mass ratio balm/cotton gauze (SCF) was varied. All experiments were performed in duplicate.

The mass of impregnated balm extract (m_{ex}) was determined gravimetrically on an analytical scale with accuracy ± 0.0001 g. Impregnation yield (I) was calculated as the mass ratio of the impregnated extract and impregnated cotton gauze/SCF (m_i) (Equation (1)).

$$I = \frac{m_{ex}}{m_i} \cdot 100\% \quad (1)$$

2.5. Re-Extraction of the Impregnated Samples

The *M. officinalis* extract was re-extracted from the impregnated materials employing an ultrasound extraction with a CHCl₃:MeOH (7:3) mixture. The samples were cut into small pieces ($\sim 3 \times 3$ mm) and rinsed in an appropriate volume of CHCl₃:MeOH (7:3) mixture to obtain the final extract concentration of approximately 1 mg/mL. The samples were sonicated using an ultrasonic bath in three cycles, each lasting for 20 min. In this way, re-extracts were prepared for chemical analyses.

2.6. Analytical Procedure

2.6.1. Gas Chromatography (GC) and Gas Chromatography/Mass Spectrometry (GC/MS)

The extracts and re-extracts were analyzed using GC and GC/MS techniques. GC/MS analyses were performed on a Shimadzu GCMSQP2010 ultra mass spectrometer fitted with a flame ionic detector and coupled with a GC2010 gas chromatograph. The InertCap5 capillary column (60.0 m \times 0.25 mm \times 0.25 μ m) was used for separation. Helium (He), at a split ratio of 1:5 and a linear velocity of 35.2 cm/s was used as a carrier gas. The ion source temperature was 200 °C, injector temperature was 250 °C, detector temperature was 300 °C, and column temperature was linearly programmed from 40 to 260 °C (at a rate of 4 °C/min), from 260 to 310 (at rate 10 °C/min) and after reaching 310 °C, kept isothermally for 10 min. The samples were dissolved in the CHCl₃:MeOH (7:3) mixture and consecutively injected in the amount of 1 μ L. The content of different compounds was determined based on the area of chromatograms and defined as content according to the GC area (the mean of three determinations). The identification of the constituents was performed by comparing their mass spectra and retention indices (RIs) with those obtained from authentic samples and/or listed in the NIST/Wiley mass-spectra libraries, using different types of searches (PBM/NIST/AMDIS) and available literature data [44].

2.6.2. High Performance Liquid Chromatography (HPLC)

Determination of rosmarinic acid was achieved using an Agilent Technologies 1200 HPLC, equipped with a Lichrospher 100RP 18e column, applying gradient elution of two mobile phases, i.e., "A/B" ("A"—0.2 M solution of phosphoric acid, and "B"—being a pure acetonitrile) at flow rates of 1 mL/min, with photodiode-array (PDA) detection (UV at 325 nm), always within 70 min. Winning combinations were 89–75% A (0–35 min); 75–60% A (35–55 min); 60–35% A (55–60 min); and 35–0% A (60–70 min). The concentrations of investigated samples were 24.72, 17.68, and 12.25 mg/mL for SFE extract, re-extract from cotton gauze, and SHF, respectively. Prior to injection, samples were filtered through polytetrafluoroethylene (PTFE) membrane filter. For the standard used in the investigation, the concentration of rosmarinic acid was 0.43 mg/mL. The volume of standard solution being injected, and that for the tested sample extracts, was 4 μ L. Identification was based on retention time and overlay curve. Once spectra matching succeeded, the result was confirmed by spiking with the respective standard to achieve a complete identification employing the so-called peak purity test. The peaks not fulfilling the requirements were not quantified. Quantification was performed by external calibration with a standard.

2.7. FTIR Analysis

ATR-FTIR spectra of the control and impregnated cotton gauze and SCF were recorded using a Nicolet™ iS™ 10 FT-IR Spectrometer (Thermo Fisher SCIENTIFIC, Darmstadt, Germany) with Smart iTR™ Attenuated Total Reflectance (ATR) Sampling accessories, within a range of 400–4000 cm^{-1} , at a resolution of 4 cm^{-1} and in 20 scan mode.

2.8. Antiviral Activity

For antiviral activity evaluation, *M. officinalis* impregnated cotton gauze with 2.24% and SCF with 8.71% impregnation yield were used. Suspensions of BHV-1 reference strain BPT-1, titer of 7.00 TCID₅₀/0.1 mL, were individually exposed to the prepared samples of *M. officinalis* impregnated materials in separate flasks for 12, 24, and 48 h.

Bovine herpesvirus 1 produces a cytopathic effect (CPE) characterized by grape-like clusters of rounded cells gathered around a hole in the monolayer after inoculation into RK-13 cell line. To determine the infectivity titer of the virus after 12, 24, and 48 h of exposure to *M. officinalis* impregnated materials, increasing dilutions of prepared samples were inoculated into the cells. Tenfold serial dilutions of each prepared sample in MEM supplemented with 2% fetal calf serum were dispensed in 96-well microtiter plate, changing pipette tips in between. Starting from the highest to the lowest, 100 μL of each dilution was transferred to 3 duplicate rows. Subsequently, 100 μL of RK—13 cell suspension was added to each well with prepared dilutions. One row containing cells inoculated with a tenfold dilution of unexposed BPR-1 strain and one row containing uninoculated cells served as a control in the experiment.

The samples were incubated at 37 °C with 5% CO₂ for 3 to 4 days and examined for the appearance of cytopathic effects (CPEs). In case no CPE was visible on day 4, the sample was considered negative for the presence of the virus. The highest dilution producing cytopathic effect in 50% of the cells, i.e., 50% end-point dilution expressed as TCID₅₀/mL, was calculated according to Reed L. and Muench H. (1938) [45].

3. Results and Discussion

3.1. Supercritical Fluid Extraction (SFE)

Selection of operating conditions for scCO₂ extraction, primary temperature, and pressure defines the properties of scCO₂ and its solvating power, thus affecting both the yield and the chemical composition of obtained extracts. Extraction of *M. officinalis* was performed at a temperature of 40 °C and pressure of 10 MPa, conditions reported as optimal to obtain essential oil components [4,15]. The kinetics of SFE processes, plotted as average values of extraction yield (y , %) vs. the amount of CO₂ consumed per amount of plant material ($m_{\text{CO}_2}/m_{\text{plant}}$, g/g) is presented in Figure 2. The literature reports low essential oil content of *M. officinalis*, ranging between 0.02% and 0.30% [46]. As can be seen from Figure 2, the yield obtained at the laboratory scale, after 3 h and a consumed scCO₂ to plant ratio of 40.25, was considerably higher (0.56%). Similarly, the yield of the first isolated fraction in supercritical scCO₂ extraction also performed at 10 MPa and 40 °C was 0.45% [37], whereas Marongiu et al. (2004) reported the amount of essential oil to be less than 0.1% at 9 MPa and 50 °C [38]. The yield of essential oil obtained by supercritical extraction in this study is also higher than that obtained by hydrodistillation, which was reported to range from 0.03% [37] to 0.41% [47,48] and similar to the yield reported for solvent-free microwave extraction (0.54%) [48].

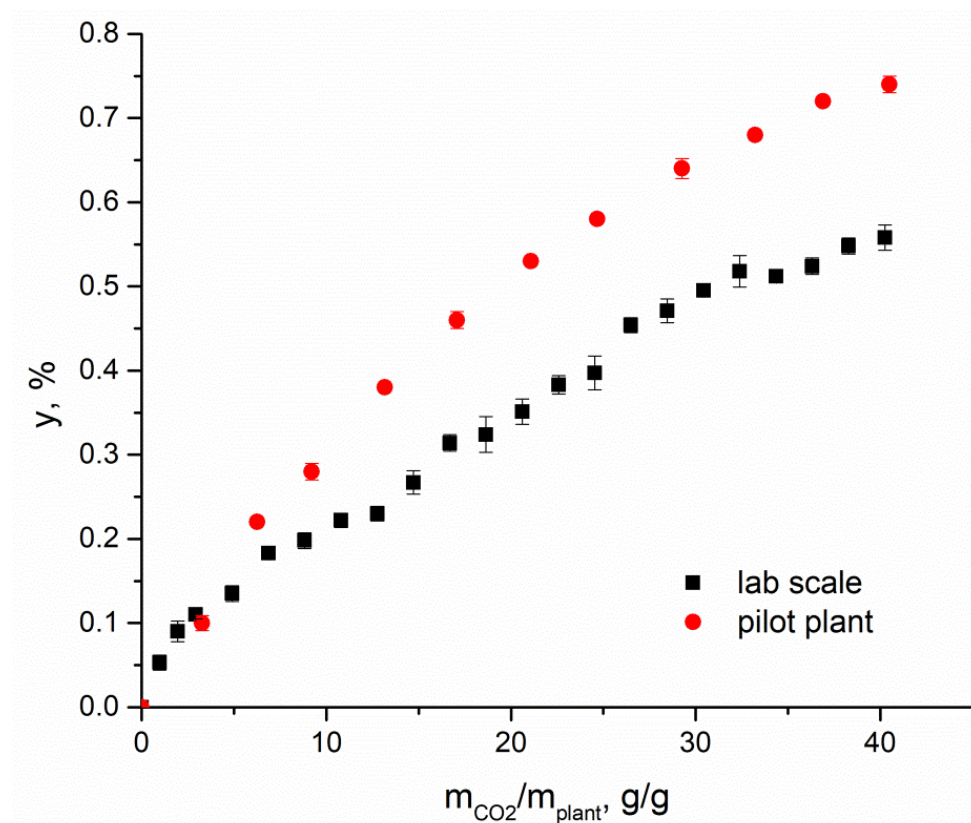


Figure 2. The yield of extract from *Melissa officinalis* vs. scCO₂ consumption at 40 °C and 10 MPa.

An important aspect in the application of SFE is the ability to predict the behavior of the process at an industrial scale from laboratory data, taking into account the differences that occur when operations are performed in equipment with significantly different dimensions [49]. Among different scale-up criteria described in the literature for SFE [50], maintaining a constant solvent to feed mass ratio and the extractor volume to plant material mass ratio (~5 for both lab and large scale) was adopted in this study. As can be seen from Figure 2, the results of laboratory and large scale, performed in 280 mL and 5 L vessels, respectively, are comparable, with the slightly higher yield achieved in the pilot-scale extraction (0.74%), while the extraction curves have similar shapes. Although literature reports on the extraction efficiency on a laboratory scale and larger scale are diverse, the results of our study are in agreement with the scale-up study reported by Prado et al. (2011), who suggested that the higher yields in pilot-scale experiments may be the consequence of the higher solvent superficial velocity, which can cause mechanical dragging of extract that is not solubilized by the scCO₂, in addition to the higher efficiency of the separators [49].

3.2. Integrated SFE-SSI Process

3.2.1. Influence of SFE-SSI Processing Mode on the Impregnation Yield of *M. officinalis* Extract into Cotton Gauze

The SFE-SSI process was carried out under the same conditions as those for SFE. A challenge in harmonizing the SFE-SSI process is to synchronize the extraction and impregnation rates by choosing the adequate processing mode regarding the throughput of CO₂ and processing time to achieve maximum extraction and impregnation yield, preventing desorption of already impregnated extract from the carrier. Four types of processing modes of the integrated SFE-SSI were performed in this study (Section 2.4) to obtain the maximal impregnation yield of balm extract on cotton gauze. Impregnation yields of *M. officinalis* extract on cotton gauze are presented in Table 1.

Table 1. Impregnation yield of *M. officinalis* extract on cotton gauze for different processing modes (40 °C, 10 MPa).

	Cycle Number	Cycle Duration, h	Total Contact Time, h/min	m_{CO_2}/m_p	$m_{ex.imp.}$, mg	I , %
Mode I	1	5	5	5.94	6.3	0.34 ± 0.035
Mode II	3	2 + 1	5/10	8.51	26.5	1.48 ± 0.127
Mode III	5	1	5/20	10.62	44.6	2.24 ± 0.141
Mode IV	7	1	7/30	12.63	16.2	0.91 ± 0.071

Before the experiments, cotton gauze was exposed to pure scCO₂ under the process conditions, using Mode I, to check for the possible presence of moisture that could affect the impregnation yield. Mass reduction of 0.3% was determined and this value was used to correct the obtained impregnation yields in the subsequent experiments.

In Mode I, after the system was filled with CO₂, the CO₂ + extract solution circulated through the extractor and adsorber vessels for 5 h. The impregnation yield obtained using this mode was only 0.34% (Table 1). In the other three modes, the process was conducted as semi-continuous, in cycles, introducing a new quantity of scCO₂ in a continuous flow between each. The duration and number of cycles were varied, as described in Section 2.4. Based on the results listed in Table 1, the introduction of fresh CO₂, accompanied by an increase in m_{CO_2}/m_p ratio, positively influenced the yield of impregnation, but only to a certain point. The highest impregnation yield (2.24%) was achieved using Mode III, which comprised five cycles with four fresh scCO₂ introductions between them. Introducing fresh scCO₂ resulted in higher specific CO₂ consumption (m_{CO_2}/m_p) while maintaining the total process time approximately equal. It enabled 6.5 times higher impregnation yield in Mode III compared to Mode I. An increased impregnation yield could be expected because the introduction of a fresh amount of CO₂ positively affects the efficiency of the extraction process [33], leading to a higher amount of balm extract in the CO₂ + extract solution, which was then available for impregnation. However, a further increase in the number of cycles and fresh CO₂ quantity, when Mode IV was applied, favored the reversible process, i.e., desorption of already impregnated *M. officinalis* extract from carrier [32,33], leading to a decrease in the impregnation yield to 0.91%. It can be concluded that five cycles and four fresh CO₂ introductions were sufficient to achieve maximum impregnation yield; therefore, Mode III was selected as optimum for *M. officinalis* extract impregnation using the integrated SFE-SSI process.

The coupled SFE-SSI process was previously applied for the impregnation of cotton gauze with *Helichrysum italicum* [36] and thyme [33] extract with 2.53% and 7.18% of impregnation yield, respectively, when processing Mode I was used (circulation of solution scCO₂ + extract for 5 h). Ivanovic et al. (2014) also tested the possibility to introduce fresh scCO₂ into the system, which enabled a higher loading yield of thyme extract (8.99%) [33]. However, in the mentioned study, depressurization of the adsorber column after each cycle was performed.

3.2.2. Influence of Plant to Carrier Mass Ratio on the Impregnation Yield of *M. officinalis* Extract

The influence of the plant to carrier mass ratio (m_p/m_c) on the impregnation yield of *M. officinalis* extract was investigated by applying Mode III, which gave the best results, under the studied conditions of 40 °C and 10 MPa. The specific CO₂ consumption ($m_{CO_2}/m_{plant} = 10.62$) and duration of the process were the same in all experiments. The impregnation yield of *M. officinalis* extract on cotton gauze increased from 1.05% to 2.24% with the increase in the plant material/cotton gauze mass ratio (Table 2) from 10 to 25, while with a further increase in m_p/m_c to 50, it remained almost the same (2.27%). Higher impregnation yield obtained with a higher plant/carrier mass ratio could be expected [24,25]. However, the impregnation is limited by the

maximal loading capacity of the material, which could be the reason why the further increase in m_p/m_c above 25 did not affect the impregnation yield.

Table 2. Influence of plant/carrier mass ratio on the impregnation yield (40 °C, 10 MPa, Mode III).

Carrier	m_p/m_c	$I, \%$
Cotton gauze	10	1.05 ± 0.092
	25	2.24 ± 0.141
	50	2.27 ± 0.205
SCF	72 (1 film)	8.71 ± 1.372
	33 (2 films)	5.44 ± 0.622

As can be seen from Table 2, high impregnation yields of *M. officinalis* extract on SCF were obtained. It should be stressed that the exposure of SCF to pure scCO₂ for 3 h under the process conditions caused no change in the SCF mass. When two films with dimensions of 120 mm × 55 mm were placed in the adsorber, which corresponded to m_p/m_c of 33, the obtained impregnation yield was 5.44%, almost 2.5 times higher than in the experiment with cotton gauze when the mass ratio of plant and carrier was comparable ($m_p/m_c = 25$). A further increase in m_p/m_c to 72 (when one film was used) enabled higher loading of 8.71%.

The higher impregnation yield obtained with SCF as a carrier than with cotton gauze can be potentially attributed to the higher affinity of the extract for SCF due to different functional groups and structural characteristics of the used materials, or to the different impregnation mechanisms for particular compounds in the extract. The impregnation efficiency depends on complex interactions between the solute, i.e., balm extract here, the mobile phase (scCO₂), and the carrier [33]. There are two different mechanisms of supercritical impregnation: the first refers to a simple deposition of a substance solubilized in supercritical fluid into the polymer matrix upon decompression, when solute remains trapped within a polymer matrix, whereas the other implies chemical interactions between the solute and polymer matrix [16,33]. Images of materials before and after impregnation are presented in Figure 3. The size and the structure of the materials did not change after impregnation, while the color of cotton gauze turned yellow, as a result of the extract impregnation. The film itself has a slightly yellowish color; thus, the color change caused by the presence of extract, in this case, was not obvious.

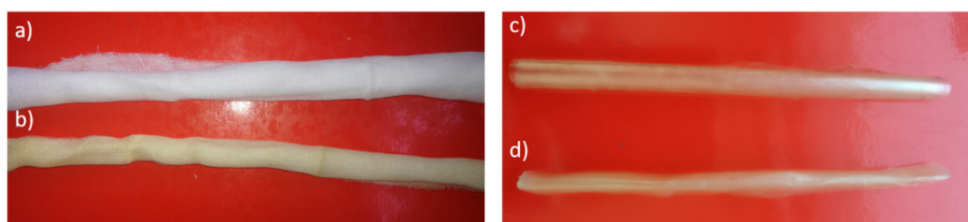


Figure 3. Images of (a) non-impregnated and (b) impregnated cotton gauze; (c) non-impregnated and (d) impregnated SCF.

Application of the SFE-SSI process for incorporation of plant extract into a polysaccharide film has not been reported in the literature yet. Impregnation of corn starch xerogels with *Helichrysum italicum* extract resulted in the loading of 1.26% at 35 MPa and 40 °C [35], and the achieved yield of thyme extract at 15 MPa and 35 °C was 1.40% [33]. Thyme extract was also loaded into chitosan gel, with an impregnation yield of only 0.96% [33]. Although the process condition and plant type influenced the obtained yield, it can be concluded that starch and chitosan materials can be successfully impregnated with plant extracts.

3.3. Chemical Profile of Extracts and Re-Extracts

The results of the GC and GC/MS analysis of *M. officinalis* extracts and re-extracts from the impregnated samples are presented in Table 3.

Table 3. Results of GC and GC/MS analysis of *M. officinalis* extracts and re-extracts from the impregnated samples (area percentage in the chromatogram, %).

	Compound	KI	SFE	Re-Extracted from Cotton Gauze	Re-Extracted from SCF
1.	hexanoic acid	975	0.42	0.55	/
2.	3E-octen-2-ol	982	0.21	0.23	/
3.	citronellal	1151	0.08	0.58	/
4.	octanoic acid	1152	t	0.97	0.09
5.	neomenthol	1161	0.2	/	/
6.	1-decen-3-ol	1177	0.13	t	t
7.	neral	1235	0.36	0.46	0.07
8.	geraniol	1249	0.14	0.23	t
9.	geranial	1268	0.57	2.57	0.13
10.	carvacrol	1298	0.19	t	0.13
11.	menthyl acetate	1302	t	t	0.2
12.	methyl geranate	1322	t	0.33	0.3
13.	neryl acetate	1353	0.29	2.99	t
14.	geranyl acetate	1358	0.31	/	/
15.	tetradecene	1391	0.13	/	/
16.	β -caryophyllene	1417	3.52	0.34	t
17.	β -(E)-farnesene	1452	0.13	0.33	t
18.	α -humulene	1472	0.25	/	/
19.	menthyl lactate	1473	t	0.44	T
20.	β -ionone	1500	0.13	/	/
21.	germacrene D	1503	0.74	0.24	t
22.	δ -cadinene	1524	t	0.24	0.56
23.	dihydroactinolide	1535	0.45	0.44	t
24.	nerolidol	1554	0.08	/	t
25.	germacren D-4-ol	1571	0.4	0.41	0.1
26.	ledol	1588	0.08	/	/
27.	caryophyllene oxide	1595	2.58	/	1.56
28.	humulene epoxide II	1610	0.15	0.39	0.08
29.	1- <i>epi</i> -cubenol	1627	0.19	0.25	0.12
30.	α -cadinol	1643	0.08	1.25	/
31.	caryophylla-4(12),8(13)-dien-5- β -ol	1661	0.16	0.39	0.18
32.	14-Hydroxy-(E)-caryophyllene	1667	0.29	/	0.32
33.	methyl tetradecanoate	1710	0.17	0.62	0.44
34.	amorpha-4,9-diene-2-ol	1713	t	0.61	0.17
35.	14-Hydroxy- α -muurolene	1756	0.18	/	/
36.	oplopanone	1745	0.3	2.2	0.55
37.	isolongifolol	1781	0.22	0.45	0.41
38.	geranylcyclopentanone	1811	0.11	0.56	0.33
39.	α -chenopodiol	1855	0.3	0.39	0.28
40.	1-hexadecanol	1882	0.31	0.8	1.66
41.	nonadecane	1900	0.2	0.87	0.61
42.	isophytol	1943	0.11	1.28	0.41
43.	hexadecanoic acid	1968	6.1	10.87	4.01

Table 3. Cont.

	Compound	KI	SFE	Re-Extracted from Cotton Gauze	Re-Extracted from SCF
44.	geranyl linalool	2031	3.03	1.76	0.14
45.	(6E,10E)-pseudophytol	2058	0.71	1.55	0.61
46.	octadecanol	2099	0.17	0.34	0.12
47.	(9Z,12Z)-octadecadienoic acid	2134	26.11	0.98	1.02
48.	docosane	2200	6.33	11.51	19.5
49.	7 α -hydroxy manool	2237	0.53	0.35	0.33
50.	isopimpinellin	2250	0.88	/	/
51.	4-epi-dehydro abietol	2320	0.11	/	/
52.	trans-ferruginol	2335	0.11	0.87	0.25
53.	tetracosane	2400	0.88	0.99	2.71
54.	hexacosane	2600	1.32	0.67	5.85
55.	heptacosane	2700	5.71	6.97	9.28
56.	octacosane	2800	0.31	5.87	0.44
57.	squalene	2835	3.63	0.42	0.97
58.	nonacosane	2900	6.33	7.9	21.35
59.	dotriacontane	3200	2.21	1.21	1.31
60.	triacontane	3000	5.67	4.46	11.91
61.	hentriacontane	3100	4.89	8.51	2.15
62.	tocopherol	3149	0.69	/	/
63.	β -sitosterol	3187	0.65	1.71	0.86
64.	ergosterol	3152	0.68	0.64	0.9
65.	dihydroergosterol	3175	0.37	0.58	0.13
66.	stigmasterol	3248	1.32	3.58	2.21
67.	(3 β ,22E)-ergosta-5,7,22-tren-3-ol acetate	3269	0.61	/	/
68.	tritriacontane	3300	4.97	4.12	2.35
69.	γ -sitosterol	3351	0.68	1.78	1.81
	Monoterpenoids		2.72	8.04	0.83
	Sesquiterpenoids		9.76	8.05	4.66
	Diterpenoids/triterpenoids		8.92	6.23	2.71
	Fatty acids and esters		32.80	13.99	5.56
	Hydrocarbons		38.95	53.08	77.46
	Phytosterols		4.31	8.29	5.91
	Other compounds		1.70	1.37	1.78
	Total		99.16	99.05	98.91

KI-Kovats index.

The GC and GC/MS analysis of the extract obtained by SFE identified 69 components representing 99.16% of the extract. The analysis revealed that alkane hydrocarbons and fatty acids and their esters were the most abundant components of the extract, at 39.1% and 32.21%, respectively. The predominant compound was linoleic acid ((9Z,12Z)-octadecadienoic acid) at 26.11%, followed by docosane (6.33%), nonacosane (6.33%), and palmitic acid (hexadecenoic acid) (6.1%). Significant amounts of sesquiterpenoids (9.76%) and diterpenoids/triterpenoids (8.92%) were also detected, among which β -caryophyllene (3.52%) and caryophyllene oxide (2.58%) were dominant. In the majority of the studies on the *M. officinalis* extract chemical composition, attention was paid to the volatile and polar constituents of the essential oil, obtained mainly by hydrodistillation technique, and dominated by the presence of oxygenated monoterpenes including citral isomers (geranial and neral), citronellal, and geraniol as the main components [4,47,51–53]. Higher amounts of fatty acids and esters (31–41%) and waxes (14–31%) were found in the extracts obtained by

scCO₂ under different process conditions [37], and in the saponifiable part of the petroleum ether soluble fraction where the presence of 80.69% of fatty acids methyl esters was determined [54]. Generally, the compositional variations in the *M. officinalis* essential oils could originate from differences in climatic, seasonal, and geographic conditions, harvesting time, and the applied extraction technique [46]. In addition, different chemical profiles between the subspecies of *M. officinalis* were also reported [55].

In the extracts obtained by re-extraction of the cotton gauze and SHF with the highest impregnation yields, 56 and 54 components were identified, comprising 99.05% and 98.91% of the extracts, respectively. The results indicated the great affinity of both cotton gauze and SHF towards hydrocarbons (waxes), which constituted 53.08% and 77.46% of the re-extracts, respectively. A significantly high content of monoterpenoids, sesquiterpenoids, and diterpenoids/triterpenoids (6.23–8.05%) was found in re-extract from cotton gauze with the highest percentage of geranial (2.57%) and neryl acetate (2.99%), followed by oplopanone, geranyl linalool, (6E,10E)-pseudophytol and isophytol. Cotton gauze also showed affinity towards palmitic acid and phytosterols, mainly stigmaterol, β -sitosterol and γ -sitosterol. Re-extract from SHF contained a noticeable amount of sesquiterpenes (4.66%) and phytosterols (5.91%), while the content of monoterpenoids was low (0.83%).

In the literature that reports the antiviral effect of balm oil, it was suggested that citral (geranial and neral) and citronellal have the main role in the antiviral activity due to the inhibition of protein synthesis in cells [4]. In addition to the mentioned oxygenated monoterpenes, rosmarinic acid was also identified as one of the components of *M. officinalis* extract assumed to be important for antiviral activity [7,12]; thus, its amount in the extract and re-extracts was determined using the HPLC method and the results are presented in Table 4.

Table 4. Content of rosmarinic acid detected in the *M. officinalis* extract and re-extracts from impregnated samples.

Sample	Rosmarinic Acid, mg/g _{extract}
SFE	0.307 ± 0.006
Re-extracted from cotton gauze	0.291 ± 0.006
Re-extracted from SCF	0.017 ± 0.000

It can be seen that the content of rosmarinic acid was relatively low, both in extract and re-extracts, compared to the literature results, where amounts between 14.7% and 80.7% were reported [56–58]. This result is not unexpected, since rosmarinic acid, as a phenolic compound, is a polar compound, and thus has low solubility in supercritical CO₂ which behaves as a non-polar solvent. Ribeiro et al. (2001) [41] and Peev et al. (2011) [59] reported the use of SFE as a pre-treatment step after which extraction of residue was performed to recover rosmarinic acid.

3.4. FTIR Analysis

FTIR analysis was carried out to evidence the presence of *M. officinalis* extract on the surface of the polymer materials, in addition to possible interactions between the extract and the matrix. FTIR spectra of pure *M. officinalis* extract, non-impregnated and impregnated cotton gauze, and SCF are presented in Figure 4. Characteristic bands of the cellulose in the neat cotton gauze (Figure 4) fit well to literature data [13,60,61]. The FTIR spectrum of the cotton gauze after impregnation shows the main differences in the range 3000–2800 cm⁻¹ and at around 1700 cm⁻¹ attributed to C–H and C=O stretching vibrations, respectively, confirming that the balm extract was effectively loaded into the gauze. The bands at 2916 and 2849 cm⁻¹ are associated with the symmetrical and asymmetrical C–H stretching vibrations of –CH₂ groups, whereas C=O vibrations at 1707 cm⁻¹ are characteristic for aldehyde and ketone groups of extract components.

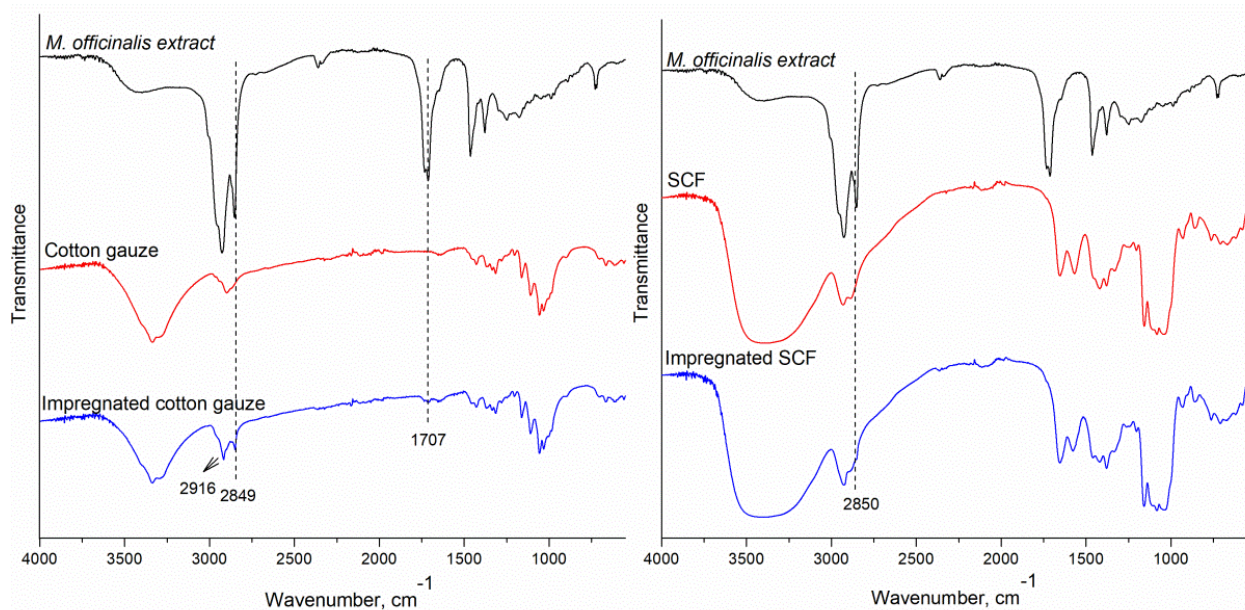


Figure 4. FTIR spectra of pure *M. officinalis* extract, non-impregnated and impregnated cotton gauze and SCF.

The FTIR spectrum of SCF shows a broad band at 3386 cm^{-1} , indicating stretching of the O–H bonds which could overlap the N–H stretching in the same region. This band can also be an indication of the development of intermolecular hydrogen bonding interactions between polymers in blend films [62,63]. The bands at 2931 and 2881 cm^{-1} are typical C–H bond stretching, whereas the bands at 1379 and 1418 cm^{-1} correspond to the C–H symmetrical deformation mode [64]. The typical region of saccharide structure is observed at 1180 – 930 cm^{-1} and comprises the stretching vibrations of C–O in C–O–H and C–O–C groups, vibration modes of C–C, and the bending mode of C–H bonds [63,65]. The amide I band in SCF originates from the stretching vibration of C=O at around 1650 cm^{-1} , and at 1568 cm^{-1} there is an amide II band due to C–N stretching vibrations in combination with N–H bending [66]. According to the literature, the band attributed to flexural vibrations of OH groups of starch (around 1661 cm^{-1}), which is overlapped with the amide I (around 1656 cm^{-1}) in chitosan, undergoes a shift to lower wavenumbers in the case of blends [62], and this shift was also observed for the amide II NH_2 absorption band at around 1550 cm^{-1} [65]. Results of FTIR analysis suggested that interactions had taken place between the hydroxyl groups of starch and the amino groups of chitosan [62–64].

The presence of *M. officinalis* extract on the surface of SCF was confirmed by the FTIR spectrum of the impregnated SCF (Figure 4). The change in the intensity of the bands in the region between 1650 and 1550 cm^{-1} indicates van der Waals interaction between the amide functionality of chitosan and the balm extract, showing that the extract was physically incorporated into the polymeric matrix, while its chemical properties were not affected by the incorporation [66]. In addition, a more intense band at 2930 cm^{-1} is observed, and a new band appeared at 2850 cm^{-1} , which originated from balm extract and can be assigned to C–H bond stretching.

In conclusion, the characteristic peaks of cotton gauze and SCF did not disappear or shift, implying that neither chemical bonding nor structural modifications occurred between the compounds from *M. officinalis* extract and the carrier during impregnation. These results indicate physical incorporation of extract that may occur due to weak molecular interactions such as Van der Waals interactions. Literature data also suggested the existence of weak interactions between polymers and extracts [13,27,67].

3.5. Antiviral Activity

After individual exposure of BHV-1 BPT-1 strain to the prepared samples of *M. officinalis* impregnated cotton gauze with 2.24% and SCF with 8.71% of the extract, for 12, 24, and 48 h, followed by titration of exposed viral suspensions, the presence of the virus in the inoculated RK-13 cell lines was not observed. In contrast, CPE was determined in control wells containing the unexposed reference strain of the virus (Figure 5).

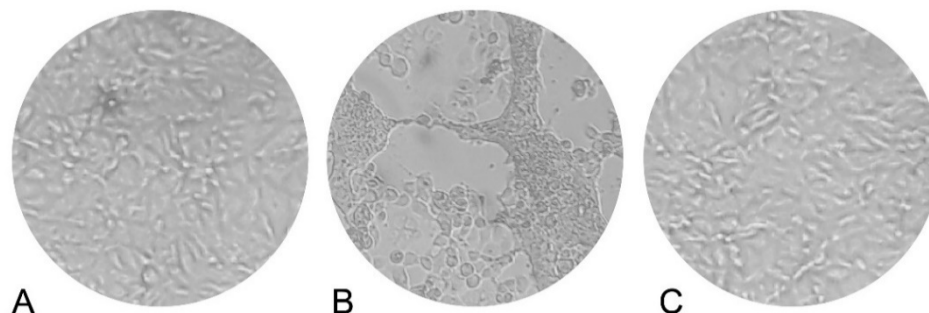


Figure 5. RK-13 cell line: (A) uninoculated cells-negative control; (B) cytopathic effect 48 h post-inoculation of unexposed BHV-1 BPT-1 strain-positive control; (C) viral suspension (dilution 10^{-6}) previously exposed to *M. officinalis* impregnated cotton gauze during 24 h.

Allahverdiyev et al. (2004) tested the antiviral activity of non-toxic concentration of *M. officinalis* volatile oil against herpes simplex virus type-2 [4]. The replication of the aforementioned virus was inhibited, indicating that the *M. officinalis* L. extract contains an anti-HSV-2 substance. The results of the investigation of Schnitzler et al. (2008) showed that *M. officinalis* oil affects HSV-1 and HSV-2 before adsorption, but not after penetration into the host cell, and further considered its suitability for topical treatment of herpetic infections [3]. Mukhtar et al. (2008) pointed out that the effects of most of the studied medicinal plants have been explored against a single member of Herpesviridae family, i.e., herpes simplex virus [6]. For example, an aqueous extract of plant material has been used to treat HSV-associated infections. The phytochemical Podophyllotoxin, isolated from the aqueous extract of *Podophyllum peltatum* L., inhibited HSV type 1. In addition to aqueous extracts, organic solvent extracts of various plants have also shown anti-HSV activity. Astani et al. (2012) determined that *M. officinalis* extract exhibits low toxicity, is virucidal, and affects HSV-1 attachment to host cells in vitro [68]. BHV-1 still causes significant economic loss to the livestock industry and trade because there are no available drugs fully effective against it. The results of our investigation indicate that after the exposure of reference BPT-1 strain of BHV-1 to prepared samples of *M. officinalis* cotton gauze and SCF in different time intervals, the presence of the virus was not observed in inoculated cells. Chemical composition analysis of re-extracts from impregnated materials revealed the presence of oxygenated monoterpenes and rosmarinic acid, compounds that were assumed in the literature to be important for the antiviral activity [4,7,12]. It was also found out that in contrast to single phenolic compounds, complex plant *Melissa* extract additionally inhibited viral attachment [68], suggesting a synergetic effect of different components of *M. officinalis* extract is responsible for its activity. Similarly, it was reported that minor components present in the essential oils can attribute to their activity against microorganisms, possibly by synergistic or antagonist effects [69]. Our results lead to the assumption that *M. officinalis* impregnated cotton gauze and film had an inhibitory effect on BHV-1, which should be thoroughly examined in future studies.

4. Conclusions

The SFE process performed at 10 MPa and 40 °C, with an achieved yield of 0.56% at the laboratory scale, was successfully transferred to the pilot-plant scale where the yield was 0.74%. Hydrocarbons, fatty acids, and their esters and terpenoids were determined to be the main constituents of the extract isolated from *M. officinalis*. The integrated SFE-SSI process

was optimized by investigation of the processing modes and plant material to solid carrier mass ratio influences on the impregnation yield at constant temperature and pressure. Both materials used in this study, cotton gauze and SCF, were successfully impregnated with components extracted from *M. officinalis* and the maximal obtained loading was 2.24% and 8.71% for cotton gauze and SCF, respectively. The results revealed that the selection of an appropriate process mode with an adequate amount of fresh CO₂ introduced into the system enabled the achievement of a high impregnation yield. The presence of *M. officinalis* extract on the surface of both materials was confirmed by FTIR analysis, and by chemical analysis of re-extracts from impregnated materials. Significant quantities of substances with reported antiviral activity, such as oxygenated monoterpenes and rosmarinic acid, were observed in the re-extracts. The *M. officinalis* impregnated materials showed an inhibitory effect on Bovine herpesvirus type 1 (BHV-1).

Author Contributions: Conceptualization, I.Z., E.S. and I.L.; Investigation, J.P., I.L., J.N., V.T. and E.V.; Formal analysis, I.Z., I.L., J.P., V.T. and J.N.; Methodology, I.Z., J.P. and I.L.; Resources, I.Z. and V.T.; Validation, I.L., J.P. and I.Z.; Writing—original draft, I.L. and J.P.; Writing—review and editing, I.Z., J.P., E.V. and I.L. All authors have read and agreed to the published version of the manuscript.

Funding: Financial support of the Ministry of Education, Science and Technological Development of the Republic of Serbia (Contract No. 451-03-68/2022-14/200135 and 451-03-68/2022-14/200287).

Institutional Review Board Statement: Not applicable.

Informed Consent Statement: Not applicable.

Data Availability Statement: The data presented in this study are available on request from the corresponding author.

Acknowledgments: Work was carried out in the frame of the COST-Action “Green Chemical Engineering Network towards upscaling sustainable processes” (GREENERING, ref. CA18224) funded by the European Commission.

Conflicts of Interest: The authors declare no conflict of interest.

References

- Whitley, R.J.; Roizman, B. Herpes simplex virus infections. *Lancet* **2001**, *357*, 1513–1518. [[CrossRef](#)]
- Akhtar, J.; Shukla, D. Viral entry mechanisms: Cellular and viral mediators of herpes simplex virus entry. *FEBS J.* **2009**, *276*, 7228–7236. [[CrossRef](#)]
- Schnitzler, P.; Schuhmacher, A.; Astani, A.; Reichling, J. *Melissa officinalis* oil affects infectivity of enveloped herpesviruses. *Phytomedicine* **2008**, *15*, 734–740. [[CrossRef](#)]
- Allahverdiyev, A.; Duran, N.; Ozguven, M.; Koltas, S. Antiviral activity of the volatile oils of *Melissa officinalis* L. against Herpes simplex virus type-2. *Phytomedicine* **2004**, *11*, 657–661. [[CrossRef](#)]
- Khan, M.T.H.; Ather, A.; Thompson, K.D.; Gambari, R. Extracts and molecules from medicinal plants against herpes simplex viruse. *Antivir. Res.* **2005**, *67*, 107–119. [[CrossRef](#)]
- Mukhtar, M.; Arshad, M.; Ahmad, M.; Pomerantz, R.J.; Wigdahl, B.; Parveen, Z. Antiviral potential of medicinal plants. *Virus Res.* **2008**, *131*, 11–120. [[CrossRef](#)]
- Nolkemper, S.; Reichling, J.; Stintzing, F.C.; Carle, R.; Schnitzler, P. Antiviral effect of aqueous extracts from species of the Lamiaceae family against Herpes simplex virus type 1 and type 2 invitro. *Planta Med.* **2006**, *72*, 1378–1382. [[CrossRef](#)]
- Geuenich, S.; Goffinet, C.; Venzke, S.; Nolkemper, S.; Baumann, I.; Plinkert, P.; Reichling, J.; Keppler, O.T. Aqueous extracts from peppermint, sage and lemon balm leaves display potent anti-HIV-1 activity by increasing the virion density. *Retrovirology* **2008**, *5*, 27. [[CrossRef](#)]
- Carvalho, F.; Duarte, A.P.; Ferreira, S. Antimicrobial activity of *Melissa officinalis* and its potential use in food preservation. *Food Biosci.* **2021**, *44*, 101437. [[CrossRef](#)]
- Dimitrova, Z.; Dimov, B.; Manolova, N.; Pancheva, S.; Ilieva, D.; Shishkov, S. Antitherpes effect of *Melissa officinalis* L. extracts. *Acta Microbiol. Bul.* **1993**, *29*, 65–72.
- Koytchev, R.; Aiken, R.G.; Dundarov, S. Balm mint extract (Lo-701) for topical treatment of recurring Herpes labialis. *Phytomedicine* **1999**, *6*, 225–230. [[CrossRef](#)]
- Mazzanti, G.; Battinelli, L.; Pompeo, C.; Serrilli, A.M.; Rossi, R.; Sauzullo, I.; Mengoni, F.; Vullo, V. Inhibitory activity of *Melissa officinalis* L. extract on Herpes simplex virus type 2 replication. *Nat. Prod. Res.* **2008**, *22*, 1433–1440. [[CrossRef](#)] [[PubMed](#)]
- Milovanovic, S.; Stamenic, M.; Markovic, D.; Radetic, M.; Zizovic, I. Solubility of thymol in supercritical carbon dioxide and its impregnation on cotton gauze. *J. Supercrit. Fluids* **2013**, *84*, 173–181. [[CrossRef](#)]

14. Jayakumar, R.; Prabakaran, M.; Sudheesh Kumar, P.T.; Nair, S.V.; Tamura, H. Biomaterials based on chitin and chitosan in wound dressing applications. *Biotechnol. Adv.* **2011**, *29*, 322–337. [[CrossRef](#)] [[PubMed](#)]
15. Reverchon, E.; De Marco, I. Supercritical fluid extraction and fractionation of natural matter. *J. Supercrit. Fluids* **2006**, *38*, 146–166. [[CrossRef](#)]
16. Kikic, I.; Vecchione, F. Supercritical impregnation of polymers. *Curr. Opin. Solid State Mater. Sci.* **2003**, *7*, 399–405. [[CrossRef](#)]
17. Khaw, K.-Y.; Parat, M.-O.; Shaw, P.N.; Falconer, J.R. Solvent Supercritical Fluid Technologies to Extract Bioactive Compounds from Natural Sources: A Review. *Molecules* **2017**, *22*, 1186. [[CrossRef](#)]
18. da Silva, R.P.F.F.; Rocha-Santos, T.A.P.; Duarte, A.C. Supercritical fluid extraction of bioactive compounds. *TrAC-Trends Anal. Chem.* **2016**, *76*, 40–51. [[CrossRef](#)]
19. Sutil, G.A.; Andrade, K.S.; Rebelatto, E.A.; Lanza, M. Effects of incorporation of pure or multicomponent active agents in biopolymers for food packaging using supercritical CO₂. *Trends. Food Sci. Technol.* **2022**, *120*, 349–362. [[CrossRef](#)]
20. Champeau, M.; Thomassin, J.M.; Tassaing, T.; Jérôme, C. Drug loading of polymer implants by supercritical CO₂ assisted impregnation: A review. *J. Control. Release* **2015**, *209*, 248–259. [[CrossRef](#)]
21. Ivanovic, J.; Milovanovic, S.; Zizovic, I. Utilization of supercritical CO₂ as a processing aid in setting functionality of starch-based materials. *Starch-Stärke* **2016**, *68*, 821–833. [[CrossRef](#)]
22. Tutek, K.; Masek, A.; Kosmalska, A.; Cichosz, S. Application of Fluids in Supercritical Conditions in the Polymer Industry. *Polymers* **2021**, *13*, 729. [[CrossRef](#)] [[PubMed](#)]
23. Goñi, M.L.; Gañán, N.A.; Martini, R.E. Supercritical CO₂-assisted dyeing and functionalization of polymeric materials: A review of recent advances (2015–2020). *J. CO₂ Util.* **2021**, *54*, 101760. [[CrossRef](#)]
24. Varona, S.; Rodríguez-Rojo, S.; Martín, Á.; Cocero, M.J.; Duarte, C.M.M. Supercritical impregnation of lavandin (*Lavandula hybrida*) essential oil in modified starch. *J. Supercrit. Fluids* **2011**, *58*, 313–319. [[CrossRef](#)]
25. Almeida, A.P.; Rodríguez-Rojo, S.; Serra, A.T.; Vila-Real, H.; Simplicio, A.L.; Delgadillo, I.; da Costa, S.B.; da Costa, L.B.; Nogueira, I.D.; Duarte, C.M.M. Microencapsulation of oregano essential oil in starch-based materials using supercritical fluid technology. *Innov. Food Sci. Emerg. Technol.* **2013**, *20*, 140–145. [[CrossRef](#)]
26. de Souza, A.C.; Dias, A.M.A.; Sousa, H.C.; Tadini, C.C. Impregnation of cinnamaldehyde into cassava starch biocomposite films using supercritical fluid technology for the development of food active packaging. *Carbohydr. Polym.* **2014**, *102*, 830–837. [[CrossRef](#)]
27. Medeiros, G.R.; Ferreira, S.R.S.; Carciofi, B.A.M. High pressure carbon dioxide for impregnation of clove essential oil in LLDPE films. *Innov. Food Sci. Emerg. Technol.* **2017**, *41*, 206–215. [[CrossRef](#)]
28. Bastante, C.C.; Silva, N.H.C.S.; Cardoso, L.C.; Serrano, C.M.; Martínez de la Ossa, E.J.; Freire, C.S.R.; Vilela, C. Biobased films of nanocellulose and mango leaf extract for active food packaging: Supercritical impregnation versus solvent casting. *Food Hydrocoll.* **2021**, *117*, 106709. [[CrossRef](#)]
29. Liparoti, S.; Franco, P.; Pantani, R.; De Marco, I. Supercritical CO₂ impregnation of caffeine in biopolymer films to produce anti-cellulite devices. *J. Supercrit. Fluids* **2022**, *179*, 105411. [[CrossRef](#)]
30. Franco, P.; Incarnato, L.; De Marco, I. Supercritical CO₂ impregnation of α -tocopherol into PET/PP films for active packaging applications. *J. CO₂ Util.* **2019**, *34*, 266–273. [[CrossRef](#)]
31. Fanovich, M.A.; Ivanovic, J.; Misic, D.; Alvarez, M.V.; Jaeger, P.; Zizovic, I.; Eggers, R. Development of polycaprolactone scaffold with antibacterial activity by an integrated supercritical extraction and impregnation process. *J. Supercrit. Fluids* **2013**, *78*, 42–53. [[CrossRef](#)]
32. Fanovich, M.A.; Ivanovic, J.; Zizovic, I.; Misic, D.; Jaeger, P. Functionalization of polycaprolactone/hydroxyapatite scaffolds with *Usnea lehariiformis* extract by using supercritical CO₂. *Mater. Sci. Eng. C* **2016**, *58*, 204–212. [[CrossRef](#)] [[PubMed](#)]
33. Ivanovic, J.; Milovanovic, S.; Stamenic, M.; Fanovich, M.A.; Jaeger, P.; Zizovic, I. Application of an Integrated Supercritical Extraction and Impregnation Process for Incorporation of Thyme Extracts into Different Carriers. In *Handbook on Supercritical Fluids, Fundamentals, Properties and Applications*; Osborne, J., Ed.; Nova Science Publishers: New York, NY, USA, 2014; pp. 257–280.
34. Zizovic, I.; Ivanovic, J.; Milovanovic, S.; Stamenic, M. Impregnations using supercritical carbon dioxide. In *Supercritical CO₂ Extraction and Its Applications*; Roj, E., Ed.; Polish Foundations of the Opportunities Industrialization Centers “OIC Poland”: Lublin, Poland, 2014; pp. 23–34.
35. Maksimović, S.; Tadić, V.; Ivanović, J.; Radmanović, T.; Milovanović, S.; Stanković, M.; Žižović, I. Utilization of the integrated process of supercritical extraction and impregnation for incorporation of *Helichrysum italicum* extract into corn starch xerogel. *Chem. Ind. Chem. Eng.* **2018**, *24*, 191–200. [[CrossRef](#)]
36. Maksimović, S.; Tadić, V.; Zvezdanovic, J.; Zizovic, I. Utilization of supercritical CO₂ in bioactive principles isolation from *Helichrysum italicum* and their adsorption on selected fabrics. *J. Supercrit. Fluids* **2021**, *171*, 105197. [[CrossRef](#)]
37. Bogdanovic, A.; Tadic, V.; Arsic, I.; Milovanovic, S.; Petrovic, S.; Skala, D. Supercritical and high pressure subcritical fluid extraction from Lemon balm (*Melissa officinalis* L., Lamiaceae). *J. Supercrit. Fluids* **2016**, *107*, 234–242. [[CrossRef](#)]
38. Marongiu, B.; Porcedda, S.; Piras, A.; Rosa, A.; Deiana, M.; Dessì, M.A. Antioxidant Activity of Supercritical Extract of *Melissa officinalis* Subsp. *officinalis* and *Melissa officinalis* Subsp. *Inodora*. *Phytother. Res.* **2004**, *18*, 789–792. [[CrossRef](#)]
39. Rozzi, N.L.; Phippen, W.; Simon, J.E.; Singh, R.K. Supercritical Fluid Extraction of Essential Oil Components from Lemon-Scented Botanicals. *LWT-Food Sci. Technol.* **2002**, *35*, 319–324. [[CrossRef](#)]

40. Angelov, G.; Penchev, P.; Condoret, J.S.; Camy, S. Optimizing the process of supercritical extraction of lemon balm (*Melissa officinalis* L.). *C. R. Acad. Bulg. Sci.* **2010**, *63*, 1141–1146.
41. Ribeiro, M.A.; Bernardo-Gil, M.G.; Esquivel, M.M. *Melissa officinalis*, L.: Study of antioxidant activity in supercritical residues. *J. Supercrit. Fluids* **2001**, *21*, 51–60. [[CrossRef](#)]
42. Pajnik, J.; Lukić, I.; Dikić, J.; Asanin, J.; Gordić, M.; Misic, D.; Zizovic, I.; Korzeniewska, M. Application of Supercritical Solvent Impregnation for Production of Zeolite Modified Starch-Chitosan Polymers with Antibacterial Properties. *Molecules* **2020**, *25*, 4717. [[CrossRef](#)]
43. Vági, E.; Balázs, M.; Komoczi, A.; Mihalovits, M.; Székely, E. Fractionation of phytocannabinoids from industrial hemp residues with high-pressure technologies. *J. Supercrit. Fluids* **2020**, *164*, 104898. [[CrossRef](#)]
44. Adams, R.P. *Identification of Essential Oil Components by Gas Chromatography/Mass Spectrometry*, 4th ed.; Allured Publishing Corporation: Carol Stream, IL, USA, 2007.
45. Reed, L.; Muench, H. A simple method of estimating fifty percent endpoints. *Am. J. Hyg.* **1938**, *27*, 493–497.
46. Shakeri, A.; Sahebkar, A.; Javadi, B. *Melissa officinalis* L.—A review of its traditional uses, phytochemistry and pharmacology. *J. Ethnopharm.* **2016**, *188*, 204–228. [[CrossRef](#)] [[PubMed](#)]
47. Jalal, Z.; El Atki, Y.; Lyoussi, B.; Abdellaoui, A. Phytochemistry of the essential oil of *Melissa officinalis* L. growing wild in Morocco: Preventive approach against nosocomial infections. *Asian Pac. J. Trop. Biomed.* **2015**, *5*, 458–461. [[CrossRef](#)]
48. Khalili, G.; Mazloomifar, A.; Larijani, K.; Tehrani, M.S.; Azar, P.A. Solvent-free microwave extraction of essential oils from *Thymus vulgaris* L. and *Melissa officinalis* L. *Ind. Crops Prod.* **2018**, *119*, 214–217. [[CrossRef](#)]
49. Prado, J.M.; Prado, G.H.C.; Meireles, M.A.A. Scale-up study of supercritical fluid extraction process for clove and sugarcane residue. *J. Supercrit. Fluids* **2011**, *56*, 231–237. [[CrossRef](#)]
50. Belwal, T.; Chemat, F.; Venskutonis, P.R.; Cravotto, G.; Jaiswal, D.K.; Bhatt, I.D.; Devkota, H.P.; Luo, Z. Recent advances in scaling-up of non-conventional extraction techniques: Learning from successes and failures. *TrAC-Trends Anal. Chem.* **2020**, *127*, 115895. [[CrossRef](#)]
51. Abdellatif, F.; Boudjella, H.; Zitouni, A.; Hassani, A. Chemical composition and antimicrobial activity of the essential oil from leaves of Algerian *Melissa officinalis* L. *EXCLI J.* **2014**, *13*, 772–781.
52. Najafian, S. Storage conditions affect the essential oil composition of cultivated Balm Mint Herb (Lamiaceae) in Iran. *Ind. Crops Prod.* **2014**, *52*, 575–581. [[CrossRef](#)]
53. Mimica-Dukic, N.; Bozin, B.; Sokovic, M.; Simin, N. Antimicrobial and Antioxidant Activities of *Melissa officinalis* L. (Lamiaceae) Essential Oil. *J. Agric. Food Chem.* **2004**, *52*, 2485–2489. [[CrossRef](#)]
54. Abdel-Naime, W.A.; Fahim, J.R.; Fouad, M.A.; Kamel, M.S. Antibacterial, antifungal, and GC–MS studies of *Melissa officinalis*. *S. Afr. J. Bot.* **2019**, *124*, 228–234. [[CrossRef](#)]
55. Basta, A.; Tzakou, O.; Couladis, M. Composition of the leaves essential oil of *Melissa officinalis* s. l. from Greece. *Flavour Fragr. J.* **2005**, *20*, 642–644. [[CrossRef](#)]
56. Caniova, A.; Brandsteterova, E. HPLC analysis of phenolic acids in *Melissa officinalis*. *J. Liq. Chromatogr. Relat. Technol.* **2001**, *24*, 2647–2659. [[CrossRef](#)]
57. Kittler, J.; Krüger, H.; Ulrich, D.; Zeiger, B.; Schütze, W.; Böttcher, C.; Krähmer, A.; Gudi, G.; Kästner, U.; Heuberger, X.; et al. Content and composition of essential oil and content of rosmarinic acid in lemon balm and balm genotypes (*Melissa officinalis*). *Genet. Resour. Crop Evol.* **2018**, *65*, 1517–1527. [[CrossRef](#)]
58. Shekarchi, M.; Hajimehdipoor, H.; Saeidnia, S.; Gohari, A.R.; Hamedani, M.P. Comparative study of rosmarinic acid content in some plants of Labiatae family. *Pharmacogn. Mag.* **2012**, *8*, 37–41.
59. Peev, G.; Penchev, P.; Penchev, D.; Angelov, G. Solvent extraction of rosemarinic acid from lemon balm and concentration of extracts by nanofiltration/Effect of plant pre-treatment by supercritical carbon dioxide. *Chem. Eng. Res. Des.* **2011**, *89*, 2236–2243. [[CrossRef](#)]
60. Chung, C.; Lee, M.E.; Choe, K. Characterization of cotton fabric scouring by FT-IR ATR spectroscopy. *Carbohydr. Polym.* **2004**, *58*, 417–420. [[CrossRef](#)]
61. Oh, S.Y.; Yoo, D.I.; Shin, Y.; Seo, G. FTIR analysis of cellulose treated with sodium hydroxide and carbon dioxide. *Carbohydr. Res.* **2005**, *340*, 417–428. [[CrossRef](#)]
62. Bof, M.J.; Bordagaray, V.C.; Locaso, D.E.; García, M.A. Chitosan molecular weight effect on starch-compositefilm properties. *Food Hydrocoll.* **2015**, *51*, 281–294. [[CrossRef](#)]
63. Ren, L.; Yan, X.; Zhou, J.; Tong, J.; Su, X. Influence of chitosan concentration on mechanical and barrier properties of corn starch/chitosan films. *Int. J. Biol. Macromol.* **2017**, *105*, 1636–1643. [[CrossRef](#)]
64. Mathew, S.; Abraham, T.E. Characterization of ferulic acid incorporated starch–chitosan blend films. *Food Hydrocoll.* **2008**, *22*, 826–835. [[CrossRef](#)]
65. Liu, H.; Adhikari, R.; Guo, Q.; Adhikari, B. Preparation and characterization of glycerol plasticized (high-amylose) starch–chitosan films. *J. Food Eng.* **2013**, *116*, 588–597. [[CrossRef](#)]
66. Silva-Pereira, M.C.; Teixeira, J.A.; Pereira-Júnior, V.A.; Stefani, R. Chitosan/corn starch blend films with extract from *Brassica oleracea* (red cabbage) as a visual indicator of fish deterioration. *LWT-Food Sci. Technol.* **2015**, *61*, 258–262. [[CrossRef](#)]
67. Dias, A.M.A.; Rey-Rico, A.; Oliveira, R.A.; Marceneiro, S.; Alvarez-Lorenzo, C.; Concheiro, A.; Júnior, R.N.C.; Braga, M.E.M.; de Sousa, H.C.J. Wound dressings loaded with an anti-inflammatory jucatá (*Libidibia ferrea*) extract using supercritical carbon dioxide technology. *J. Supercrit. Fluids* **2013**, *74*, 34–45. [[CrossRef](#)]

-
68. Astani, A.; Reichling, J.; Schnitzler, P. *Melissa officinalis* extract inhibits attachment of herpes simplex virus in vitro. *Chemotherapy* **2012**, *58*, 70–77. [[CrossRef](#)]
 69. Perumal, A.B.; Huang, L.; Nambiar, R.B.; He, Y.; Li, X.; Sellamuthu, P.S. Application of essential oils in packaging films for the preservation of fruits and vegetables: A review. *Food Chem.* **2021**, *375*, 131810. [[CrossRef](#)]